Computations of Light-Scattering and Extinction by Spheres According to Diffraction and Geometrical Optics, and Some Comparisons with the Mie Theory

J. R. HODKINSON* AND I. GREENLEAVES
Medical Research Council, London School of Hygiene and Tropical Medicine
(Received 16 July 1962)

The scattering and extinction of light by systems of transparent, spherical particles have been calculated on the basis of classical diffraction and of geometrical scattering by external reflection and transmission, for the refractive index range 1.1 to 2.0 and scattering angles up to about 40°, and presented as a set of graphs for general use. Provided that the particles are larger than 3 or 4 wavelengths of light, and that there is a sufficient range (say 2:1) of particle sizes present to average out effects of phase, the scattering and extinction calculated in this way agree well with such direct calculations by the Mie theory as are at present available. It is thought that the treatment should also be successful with irregular particles, and to some extent with nontransparent ones, such as often occur in airborne dusts in industry. The conditions under which scattering and extinction measurements can be used to estimate the surface-area of particles in suspension in air or liquid are discussed.

1. INTRODUCTION

WHEN particles are larger than a few wavelengths of light, and a range of particle sizes or illuminating wavelengths is present, their combined light scattering, and consequently their extinction, may be treated approximately as a combination of classical diffraction and of geometrical transmission and reflection.[1–5] This simplifies the computations very considerably in comparison with the rigorous electromagnetic treatment of the Mie theory,[6] and a further simplification is possible by the approximation methods of Ellison and Peetz[7] for calculating the geometrical scattering. Even so, the amount of computation needed adequately to illustrate the phenomena over a wide range of refractive index is considerable. Such calculations have been made to give guidance on the choice and interpretation of light scattering and extinction measurements on dusts. It is thought that their presentation in graphical form will be of general interest, as well as of direct assistance to those with similar problems.

The calculations cover the refractive-index range 1.1 to 2.0 and scattering angles up to about 40°. They largely follow the methods of Ellison and Peetz,[5] whose criterion of approximation is a maximum error of 0.01 in the apparent extinction coefficients or about 1% in the scattered intensity, compared with calculations of geometrical scattering from exact formulae.

* Now in Department of Radiation Biology, University of Rochester, New York.

[1] J. Bricard, J. Phys. Radium 4, 57–65 (1943).
[2] J. Bricard, Ann. Geophys. 2, 231–248 (1946).
[3] J. McK. Ellison, "The Scattering of Light by Dusts and Its Application to the Evaluation of Industrial Dust Clouds," Ph.D. thesis, London University, 1954.
[4] J. McK. Ellison, Brit. J. Appl. Phys. Suppl. 3, 66–71 (1954).
[5] J. McK. Ellison, Proc. Phys. Soc. (London) **B70**, 102–111 (1957).
[6] H. C. Van de Hulst, *Light Scattering by Small Particles* (John Wiley & Sons, Inc., New York, 1957).
[7] J. McK. Ellison and C. V. Peetz, Proc. Phys. Soc. (London) **B74**, 105–123 (1959).

2. CALCULATIONS

2.1 Concept of Scattered-Intensity Coefficient, $I(\theta,d)$

The intensity coefficient $I(\theta,d)$ of light scattered at a given angle θ from the direction of propagation of the incident plane wavefront is defined as the light flux per unit solid-angle scattered in the direction θ divided by the flux geometrically incident on the particle, i.e. by the product of the illumination (flux per unit area) and the cross-sectional area of the particle $\pi d^2/4$. It is calculated as though it arose from the diffraction [intensity $I_0(\theta,d)$] of light passing near the particle, and from the external reflection [intensity $I_1(\theta)$] and transmission [intensity $I_2(\theta)$] of light incident on the particle, according to the laws of geometrical optics. Absorption must be allowed for if the particle is not perfectly transparent. Internal reflection is negligible, except at the angles where rainbows are formed. The phase of the geometrical-optics components I_1 and I_2 is neglected because we are considering systems where the particle size-range is wide enough to average out phase effects. The angular distribution of the geometrical components is the same for all particle sizes and the total light flux scattered through a given solid angle is proportional to the total flux incident on the particle, i.e. to its projected area. Hence, the geometrical intensity coefficients I_1 and I_2 as here defined are independent of particle size. The diffraction component I_0 varies with the particle size. That is,

$$I(\theta,d)=I_0(\theta,d)+I_1(\theta)+I_2(\theta).$$

2.2 Scattering due to Diffraction

The diffracted intensity $I_0(\theta,d)$ is independent of refractive index and is readily calculated from the usual formula

$$I_0(\theta,d)=\frac{\alpha^2}{4\pi}\left(\frac{2J_1(\alpha\sin\theta)}{\alpha\sin\theta}\right)^2=\frac{J_1^2(\alpha\sin\theta)}{\pi\sin^2\theta}, \qquad (1)$$

where $\alpha=\pi d/\lambda$, d = particle diameter, λ = wavelength of

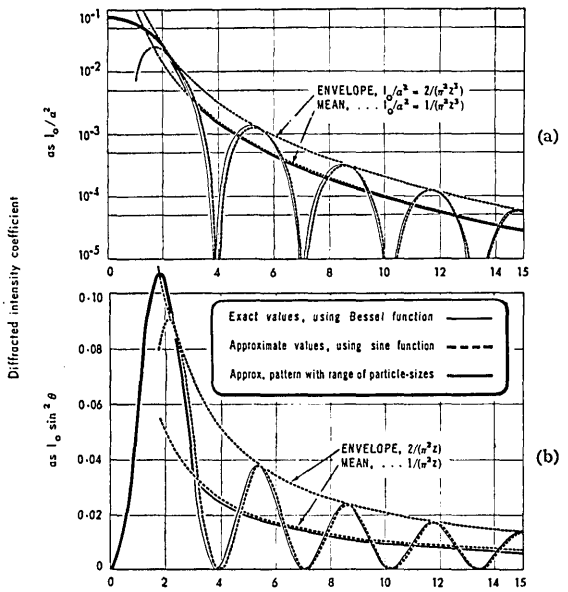

FIG. 1. Distribution of intensity diffracted by spheres vs diffraction parameter, $z=\alpha \sin\theta$. (a) Variation with angle for a given particle size. (b) Variation with particle size for a given angle.

light, and provided that θ is not too large, so that $\sin\theta \doteqdot \theta$. For larger values of θ the intensity so calculated must be multiplied by a factor $k=\frac{1}{2}(1+\cos^2\theta)$,[8] which at $\theta=30°$, for example, is 0.875. To provide a graph of general application, $I_0/\alpha^2=[2J_1(z)/z]^2/4\pi$ may be plotted against the diffraction parameter $z=\alpha \sin\theta$ [Fig. 1(a)]. It is readily seen that the diffracted intensity coefficient varies rapidly with angle for particles of a given size.

If, however, we wish to visualize the variation in diffracted intensity coefficient for a given angle, as the particle size varies, it is more appropriate to plot $I_0 \sin^2\theta = J_1^2(z)/\pi$ against z [Fig. 1(b)]; this form is in any case more convenient for calculation. For values of z beyond the first intensity minimum, the mean level of intensity scattered through a given angle does not vary rapidly with particle size.

For values of $z>4\pi$ the first-order Bessel function approximates closely to a damped sine-function

$$Lt_{z\to\infty} J_1(z) = (2/\pi)^{\frac{1}{2}} \sin(z-\pi/4).$$

We may then write

$$I_0/\alpha^2 \doteqdot (2/\pi^2 z^3)\sin^2(z-\pi/4),$$

which has been plotted on Fig. 1(a) for comparison with the Bessel-function expression. Although the discrepancies at a particular value of z become appreciable for $z<11$ and considerable for $z<8$, this is chiefly due to displacement of the maxima and minima. The general form of the two curves is the same down to $z=2\frac{1}{2}$, well within the first lobe. For $z<2\frac{1}{2}$ the approximation breaks down because $Lt_{z\to\pi/4} \sin(z-\pi/4)=0$, whereas $Lt_{z\to 0}[J_1(z)/z]=\frac{1}{2}$. The envelope of the sine expression, $I_0/\alpha^2=2/(\pi^2 z^3)$, is a good fit to the Bessel-function expression.

In the presence of a sufficient range of particle size, 2:1 or more, only the main diffraction maximum is seen, the higher-order maxima being smoothed out by the superposition of the patterns of particles of different size. In that case the distribution of I_0/α^2 outside the forward maximum will be represented approximately by the mean of the sine expression, i.e. by $I_0/\alpha^2=1/(\pi^2 z^3)$, where α and z take the values appropriate to the root-mean-square diameter of the particles. Within the forward lobe formula (1) must of course be used.

We may also write, using the sine approximation,

$$I_0 \sin^2\theta \doteqdot (2/\pi^2 z)\sin^2(z-\pi/4),$$

which is shown in Fig. 1(b) for comparison with the Bessel-function expression. Outside the first lobe of the diagram, the variation of diffracted-intensity coefficient with root-mean-square particle diameter is given by $I_0 \sin^2\theta = 1/(\pi^2 z)$, provided there is at least a 2:1 range of sizes present.

For the comparisons with the Mie theory given below (Sec. 4), the diffraction has been calculated from the

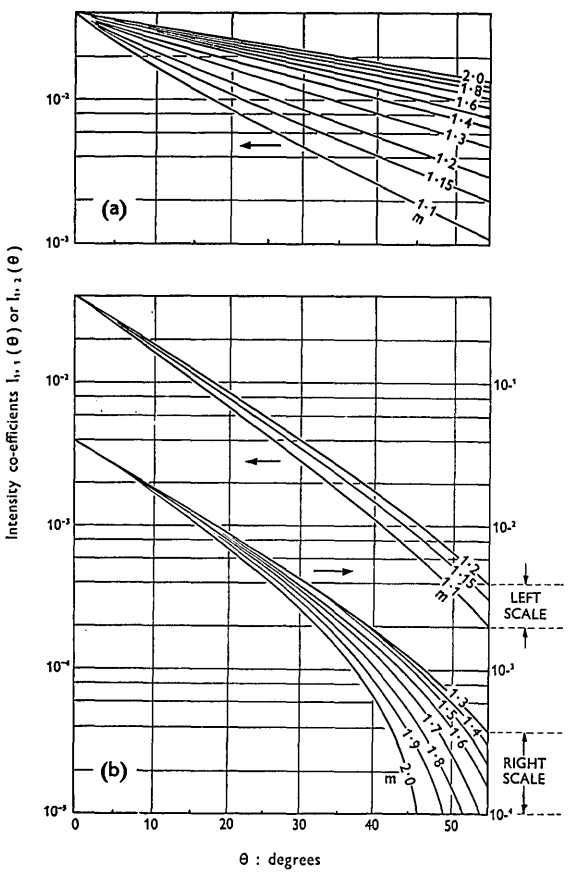

FIG. 2. Angular distribution of light scattered by external reflection from a particle for refractive indices 1.1 to 2.0. (a) Polarization 1, $I_{1,1}(\theta)$. (b) Polarization 2, $I_{1,2}(\theta)$.

[8] C. Wiener, Abhandl. Kaiserl. Leopold. Karol. Deut. Akad. Naturforsch. 13, 1 (1907).

TABLE I. Scattering by a transparent sphere due to external reflection, calculated by geometrical optics.

Upper and lower rows for each angle give polarized components $I_{1,1}(\theta)$ and $I_{1,2}(\theta)$ of scattered-intensity coefficient $I_1(\theta)$, flux scattered per unit solid angle in direction θ per unit geometrically incident flux, $\times 10^4$.

Scattering angle θ, (deg)	Refractive index										
	1.1	1.15	1.2	1.3	1.4	1.5	1.6	1.7	1.8	1.9	2.0
0°	398	398	398	398	398	398	398	398	398	398	398
	398	398	398	398	398	398	398	398	398	398	398
5°	273	295	308	330	337	343	349	353	356	360	360
	252	265	270	275	283	280	280	275	270	269	270
10°	186	215	235	262	278	293	303	311	318	319	328
	159	179	186	193	198	196	193	189	186	182	178
15°	131	160	181	212	233	250	263	274	282	297	297
	100	117	129	137	136	136	133	131	126	121	117
20°	90.5	120	142	174	194	214	228	240	250	260	268
	63.5	77.5	86	95	93.5	94	90.5	83.5	81	78	72
25°	65	90	110	143	166	183	199	211	225	225	241
	40.3	50.8	58.1	64	65	63.5	61	56	54	53.0	45
30°	47	68.2	86.5	117	141	160	174	187	200	207	218
	25.0	34.0	39.8	43	45	42.5	40.1	37	33	29.2	26.5
35°	33.8	52.4	69.5	96.5	119	140	154	168	180	189	199
	16	22.2	26	29	29.0	28.5	24.2	22	19	15.7	14.0
40°	25.2	40.5	55	79	101	120	136	150	161	172	181
	10.2	14.5	17	18.7	18.4	17.5	14.8	12.8	10.5	8	6.8
45°	18.7	32.5	45.5	67	86.5	102	119	133	146	157	166
	6.36	9.5	10.5	11.7	11.1	10.0	8.01	6.8	4.79	3.3	1.8
50°	14.6	25.5	36	56.5	72.5	91	105	119	131	148	152
	3.90	5.7	6.45	7.02	6.30	5.27	3.89	2.60	1.62	0.9	11.5
55°	11.4	20.4	29.8	48	65.5	80	93.8	106	119	130	139
	2.18	3.20	3.78	3.84	3.22	2.36	1.46	0.743	0.201	0.006	3.45
60°	9.05	16.1	24.5	40.5	57.5	70.5	83.5	95.8	107	118	128
	1.27	1.63	2.02	1.89	1.33	0.745	0.25	0.05	0.156	0.96	0
70°	5.98	11.4	17.3	30.3	43.2	56	67.5	78.8	88.5	99	108
	0.324	0.382	0.354	0.165	0.025	0.0825	0.56	1.3	2.15	3.4	5.2
80°	4.18	8.18	12.7	23.1	33.8	45	55.5	65.5	75	84.0	93.2
	0.023	0.009	0.093	0.24	0.51	1.27	2.5	4.2	6.0	8.2	10.6
90°	3.03	6.08	9.68	18.0	27.3	36.8	46.5	55.5	63.5	72.5	80.8
	0.020	0.094	0.235	0.78	1.85	3.22	5.0	7.8	10.6	13.5	16.6
100°	2.25	4.78	7.65	14.6	22.4	31.0	39.0	47.8	56	64	71.8
	0.147	0.365	0.75	1.87	3.54	5.60	8.75	11.7	14.9	18.3	22.0
110°	1.82	3.83	6.2	12.1	20.0	26.5	33.8	41.8	49.5	57	64.0
	0.307	0.684	1.29	2.9	5.21	7.88	11.6	15.1	19.1	23.0	27.3
120°	1.50	3.20	5.2	10.4	16.4	23.1	30.0	36.8	44.5	51.2	59.5
	0.454	0.995	1.78	3.85	6.75	9.92	13.9	18.1	22.6	26.9	32.0
130°	1.28	2.70	4.52	9.1	14.5	20.6	27.0	33.5	39.9	47.i	54
	0.59	1.27	2.23	4.72	8.03	11.7	16.1	20.7	25.8	30.2	35.4
140°	1.13	2.37	4.00	8.2	13.1	18.7	24.6	30.9	37.2	43.8	50
	0.70	1.51	2.63	5.40	9.15	12.3	18.0	22.9	28.5	33.2	38.7
150°	1.02	2.14	3.68	7.55	11.0	17.4	23.1	29.1	35.5	41.2	47.5
	0.788	1.69	2.94	6.03	10.1	14.4	19.4	24.3	30.1	35.3	41.2
160°	0.98	2.00	3.45	7.05	11.5	16.5	22.1	27.8	33.7	39.4	46
	0.850	1.82	3.14	6.53	10.6	15.2	20.4	25.7	31.5	37.0	42.8
170°	0.95	1.97	3.32	6.8	11.2	16.1	20.1	27.1	32.8	38.6	45
	0.785	1.90	3.27	6.8	10.9	15.6	21.0	26.4	32.5	37.8	43.8
180°	0.92	1.93	3.28	6.78	11.0	15.2	21.2	26.8	32.5	38.2	44.5
	0.888	1.93	3.31	6.90	11.0	15.6	21.1	26.7	32.5	38.2	44.2

exact formula, since this did not involve much labor. In practice, however, the sine approximation may save a great deal of labor and gives adequate accuracy, especially since, outside the first diffraction lobe, the diffracted intensity is much smaller than the refracted or reflected intensities. At wide angles the obliquity factor $\frac{1}{2}(1+\cos^2\theta)$ must be used with the sine approximation as with the exact expression (1).

At angles so wide that $\theta \doteqdot \sin\theta$ is no longer approximately true, a better approximation is obtained if z is defined as $\alpha\theta$ instead of $\alpha \sin\theta$, both in the exact formula (1) and in the sine approximation (6).

2.3 Scattering due to External Reflection, $I_1(\theta)$

The externally reflected component of the geometrical scattering $I_1(\theta)$ is resolved into components $I_{1,1}(\theta)$ and $I_{1,2}(\theta)$ polarized, respectively, in and normal to the plane containing the incident and scattered rays. The component $I_{1,1}(\theta)$ (Fig. 2 and Table I) has been computed for a range of refractive indices by the exact formula

$$I_{1,1}(\theta)=\frac{1}{8\pi}\left\{\frac{\sin(\theta/2)-[m^2-1+\sin^2(\theta/2)]^{\frac{1}{2}}}{\sin(\theta/2)+[m^2-1+\sin^2(\theta/2)]^{\frac{1}{2}}}\right\}^2, \quad (2)$$

TABLE II. Scattering by a transparent sphere due to transmission with two refractions, calculated by geometrical optics.[a]

Body of table: Scattered-intensity coefficient $I_2(\theta)$, flux scattered per unit solid angle in direction θ per unit geometrically incident flux.

Scattering angle θ, (deg.)	Refractive index 1.1	1.15	1.2	1.3	1.4	1.5	1.6	1.7	1.8	1.9	2.0
0	9.59	4.63	2.82	1.44	0.922	0.660	0.507	0.408	0.340	0.290	0.251
5	6.51	3.81	2.50	1.36	0.891	0.646	0.498	0.404	0.337	0.288	0.250
10	2.82	2.38	1.85	1.16	0.807	0.602	0.476	0.388	0.326	0.280	0.244
15	1.14	1.29	1.22	0.916	0.691	0.540	0.437	0.363	0.310	0.269	0.236
20	0.470	0.679	0.750	0.682	0.570	0.470	0.392	0.333	0.288	0.253	0.224
25	0.203		0.457	0.492	0.452	0.389	0.344	0.299	0.264	0.235	0.211
30			0.273	0.347	0.348	0.324	0.293	0.265	0.236	0.215	0.195
35			0.153	0.241	0.264	0.260	0.245	0.228	0.211	0.195	0.179
40			0.0921	0.163	0.197	0.207	0.203	0.196	0.184	0.173	0.164
45			0.0505		0.146	0.162	0.166	0.164	0.160	0.152	0.144
50			0.0232			0.125	0.133	0.136	0.136	0.133	0.128
55			0.0092				0.106	0.113	0.114	0.114	0.111
60			0.00188							0.0962	0.0957

[a] Polarized components are calculable from relation $I_2 = I_{2,1} + I_{2,2} = I_{2,1}(1 + \sec^4\theta)$. Values above single-dotted lines are calculated from Ellison and Peetz[7] approximation. Values below double-dotted lines may be overshadowed by rainbows.

where m = particle refractive index (complex if the particle is not perfectly transparent). The approximate formula of Ellison and Peetz[7] was not used because it saves little labor. For angles $\theta > 55°$, not shown in Fig. 2, the curves flatten and become horizontal at $\theta = 180°$.

The component $I_{1,2}(\theta)$ has also been computed by the exact formula

$$I_{1,2}(\theta) = \frac{1}{8\pi}\left\{\frac{m^2\sin\theta/2 - (m^2 - 1 + \sin^2\theta/2)^{\frac{1}{2}}}{m^2\sin\theta/2 + (m^2 - 1 + \sin^2\theta/2)^{\frac{1}{2}}}\right\}^2. \quad (3)$$

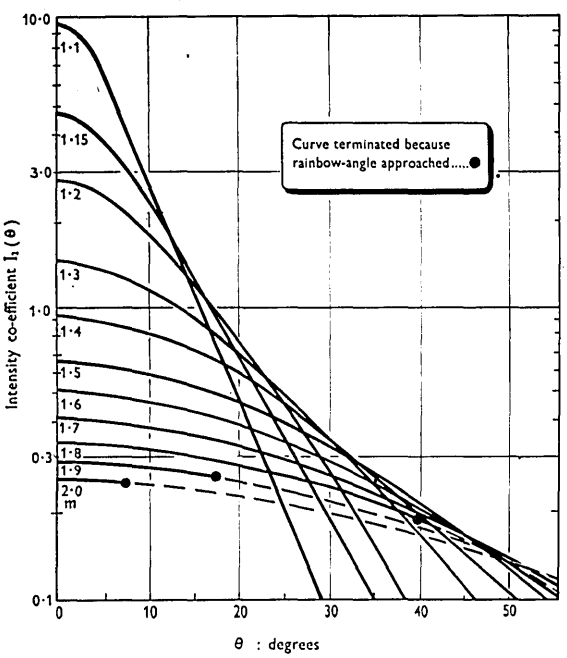

FIG. 3. Angular distribution of light scattered by transmission through a particle, sum of both polarizations for refractive indices 1.1 to 2.0.

The approximate formula of Ellison and Peetz[7] involves considerable errors.

It is seen that $I_{1,2}(\theta)$ falls to zero when $\tan\frac{1}{2}\theta = 1/m$, corresponding to rays incident on the surface of the sphere at the Brewster angle, and then increases at higher angles. Figure 2 does not extend to these angles (e.g., the curve for $m = 2$ does not fall to zero until $\theta = 63.2°$). At any given lower angle, $I_{1,2}$ shows a maximum at a refractive index given by $m^2 = 2(1 - \sin^2\theta/2)$. At angles of 10°, 30°, and 50° the intensity is a maximum for refractive indices 1.41, 1.37, and 1.28, respectively.

Both $I_{1,1}(\theta)$ and $I_{1,2}(\theta)$ are of course independent of particle size.

2.4 Scattering due to Transmission with Refraction, $I_2(\theta)$

The exact formula for the transmitted-intensity coefficient is

$$I_2(\theta) = \frac{2}{\pi}\left(\frac{m}{m^2-1}\right)^4 \frac{(m\cos\theta/2 - 1)^3(m - \cos\theta/2)^3}{\cos\theta/2\,(m^2 + 1 - 2m\cos\theta/2)^2} \times\left(1 + \sec^4\frac{\theta}{2}\right). \quad (4)$$

In the final bracket the term 1 corresponds to the polarized component $I_{2,1}(\theta)$, and $\sec^4\theta/2$ to $I_{2,2}(\theta)$. Only $I_2(\theta)$ need be computed, therefore, since the components are readily found from it by means of the relationships $I_{2,1} = I_2/(1 + \sec^4\theta/2)$ and $I_{2,2} = I_2\sec^4\theta/2/(1 + \sec^4\theta/2)$. Since, as θ increases from 0° to 40°, $\sec^4\theta/2$ increases only from 1 to 1.28, $I_2(\theta)$ is not so strongly polarized as the reflected component $I_1(\theta)$. Ellison and Peetz's[7] approximations involve less labor than formula (4) and

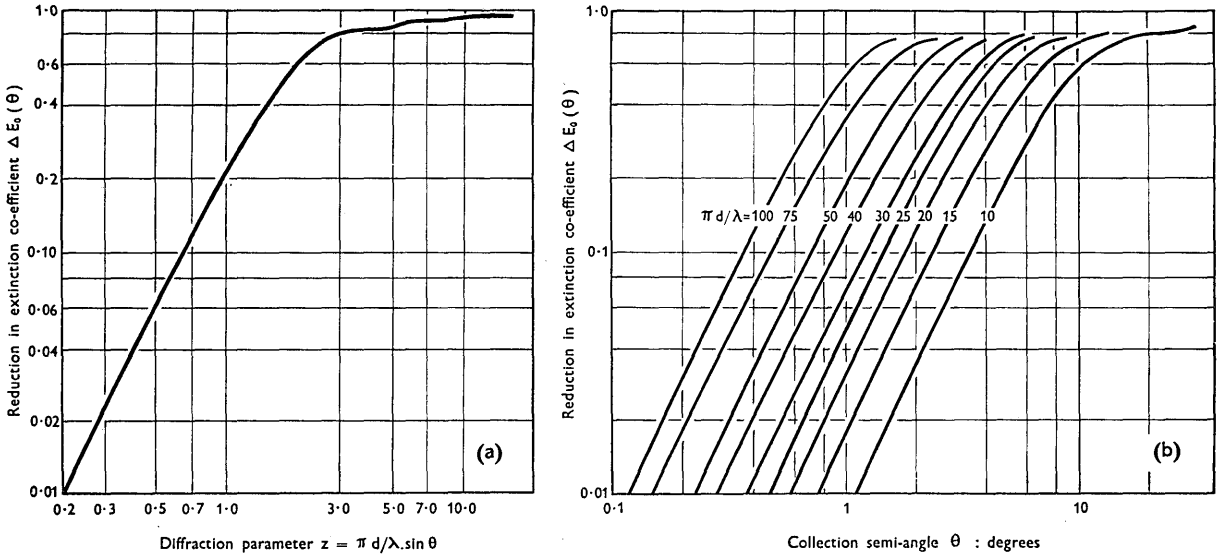

FIG. 4. Reduction in extinction coefficient due to collection of diffracted light. (a) As function of diffraction parameter $z=\pi d/\lambda \sin\theta$, where d=particle diam, θ=semiangle of collected cone, and λ=wavelength of light. (b) As function of collecting semiangle θ for various particle sizes.

have been used here to calculate the values of $I_2(\theta)$ (Fig. 3 and Table II). The exact formula (4) has been used where necessary to maintain $\pm 1\%$ accuracy in $I_2(\theta)$ at the larger angles, especially at the lower refractive indices. The curves for refractive indices 1.7 to 2.0 have been curtailed at angles in proximity to rainbows arising from light reflected twice inside the particle, because they give rise to intensity maxima whose magnitude cannot be calculated from geometrical optics, and recourse must be made to the Mie theory,[6] even though there may be a sufficient range of particle size present to average out the size-dependent interference effects. $I_2(\theta)$ is otherwise independent of particle size.

2.5 Concept of Light Extinction Coefficient, E

We define the extinction coefficient E of a particle illuminated by parallel light as the ratio of the total flux scattered and absorbed to the total flux geometrically incident on the particle. On classical optics the extinction coefficient has the value two, comprising equal contributions of unity from light experiencing reflection, transmission, or absorption, and from light diffracted by the particle (Babinet's principle)[9], i.e.,

$$E=2\pi\int_0^\pi I(\theta)\sin\theta d\theta=2\pi\int_0^\pi I_0(\theta,d)\sin\theta d\theta + 2\pi\int_0^\pi [I_1(\theta)+I_2(\theta)]\sin\theta d\theta,$$

where

$$2\pi\int_0^\pi I_0(\theta,d)\sin\theta d\theta=2\pi\int_0^\pi \{I_1(\theta)+I_2(\theta)\}\sin\theta d\theta=1.$$

[9] W. A. Walton, Trans. Inst. Chem. Engrs. (London) 25, Suppl. "Particle Size Analysis," 141–142 (1947).

In practice some of the scattered light is collected due to the finite angle subtended at the particle by the receiver. The observed extinction coefficient is then less than 2 by an amount $\Delta E(\theta)$ which may be regarded as the sum of three components: $\Delta E_0(\theta)$ due to collection of some of the light scattered by diffraction, $\Delta E_1(\theta)$ due to collection of some of the light scattered by external reflection, and $\Delta E_2(\theta)$ due to collection of some of the light scattered by transmission and refraction, where θ is the semiangle of the cone of light collected.

The decrease in the amount of light falling as a parallel beam on a receiver which subtends a semiangle θ at a particle in the beam, owing to the presence of the particle, is thus

$$\frac{\pi^2 d^2}{2}\int_\theta^\pi I(\theta,d)\sin\theta d\theta=\frac{\pi d^2}{4}\left\{E-2\pi\int_0^\theta I_0(\theta,d)\sin\theta d\theta - 2\pi\int_0^\theta [I_1(\theta)+I_2(\theta)]\sin\theta d\theta\right\}$$
$$=\frac{\pi d^2}{4}[2-\Delta E_0(\theta,d)-\Delta E_1(\theta)-\Delta E_2(\theta)].$$

Departure from parallelism of the incident beam, due to the finite angle subtended at the particle by the light source, also causes the extinction to be less than E, but by an amount which cannot readily be calculated. Very nearly parallel beams are therefore essential in quantitative light-extinction experiments.

2.6 Reduction in Extinction Coefficient due to Collection of Some Diffracted Light, $\Delta E_0(\theta)$

The reduction in extinction due to the collection by the receiver of a finite cone of semiangle θ of the light

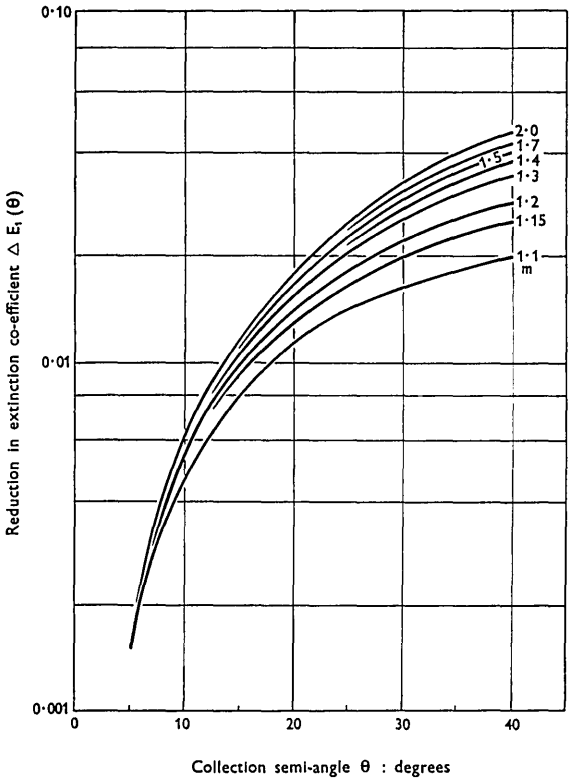

FIG. 5. Reduction in extinction coefficient due to light externally reflected from the particle, for refractive indices 1.1 to 2.0.

diffracted by a particle illuminated by a parallel beam is found by integration of the diffraction formula for the angular distribution of diffracted intensity, giving

$$\Delta E_0 = 2 - J_0^2(\alpha \sin\theta) + J_1^2(\alpha \sin\theta). \qquad (5)$$

This is plotted in Fig. 4, and is of course independent of refractive index.

2.7 Reduction in Extinction Coefficient due to Collection of Some Externally Reflected Light, $\Delta E_1(\theta)$

The reduction in extinction due to the collection of a finite cone of semiangle θ of the externally reflected light by the receiver is found by integration of the formulas (2) and (3) above. Ellison and Peetz's[7] approximate formula can be in error by up to several percent, especially at the larger angles. However, since the externally reflected intensity is usually one-tenth or less of the diffracted or transmitted intensity, the resulting error in the total reduction in extinction, $\Delta E(\theta)$, is less than 1%. The variation of $\Delta E_1(\theta)$ with θ is plotted in Fig. 5 for various values of refractive index m; it is, of course, independent of particle diameter.

2.8 Reduction in Extinction due to Collection of Some Transmitted and Refracted Light, $\Delta E_2(\theta)$

The reduction in extinction due to the collection of a finite cone of semiangle θ of the transmitted and refracted light is found by integration of the formula (4) above. The approximations of Ellison and Peetz here give an accuracy of about $\pm 1\%$ and have been used to calculate the values of $\Delta E_2(\theta)$ which are plotted in Fig. 6.

3. USE OF THE GRAPHS

Some examples of the use of these graphs are now given.

3.1 Scattering Measurements on Transparent Spheres

Suppose we wish to predict the intensity of light scattered through an angle $\theta = 15°$ by a suspension of transparent spheres of refractive index 1.5 ranging in diameter from 2 to 3.6 μ. To simplify the calculation we shall assume the size-distribution of the spheres to be such that equal increments of particle diameter d give equal increments of particle projected area, i.e., the frequency of particles of diameter d is proportional to $1/d^2$; and that the wavelength λ of the incident light is $0.2\pi = 0.61\ \mu$. The particle-size parameter $\alpha = \pi d/\lambda$ thus ranges from 10 to 18.

First, the scattering I_0 due to diffraction, which varies with particle size, must be obtained from Fig. 1 and averaged over the whole particle-size range. If we read from Fig. 1 the values of $I_0(\theta)/\alpha^2$ for each of the nine size parameters $\alpha = 10, 11, 12, \ldots 18$, i.e., of the diffraction parameter $\alpha \sin\theta = 2.59, 2.85, 3.11, \ldots 4.66$, multiply each value by α^2 to get $I_0(\theta)$, and average

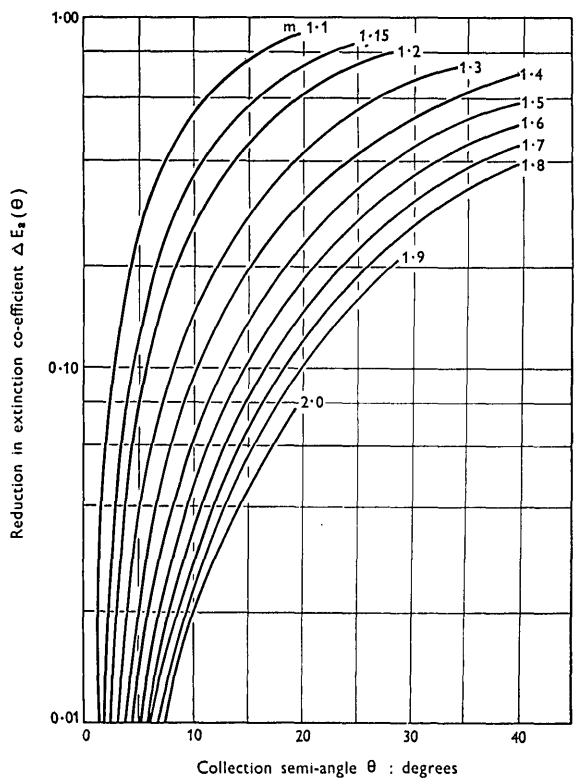

FIG. 6. Reduction in extinction coefficient due to collection of light transmitted through a particle, for refractive indices 1.1 to 2.0.

them, we find a mean value 0.338 for I_0 (15°). If the particle-size distribution were other than we have assumed, it would be necessary in averaging to weight each of the nine contributions to $I_0(\theta,d)$ according to the proportion of particle projected area falling in the corresponding increment of α. In fact, the assumption of a particle-diameter frequency proportional to $1/d^2$ gives a type of size distribution similar to many that are found in practice with polydisperse systems, especially with ground materials, in that the finer particles are the more numerous.[10]

Next the scattered intensity due to external reflection for $m=1.5$, $\theta=15°$ is read from Fig. 2, $I_1=I_{1,1}+I_{1,2}=0.025+0.014=0.039$; and that due to transmission is read from Fig. 3, $I_2=0.540$.

The total light flux per unit solid angle scattered through an angle of 15° is thus $I=I_0+I_1+I_2=0.338+0.039+0.540=0.917$ of the flux geometrically incident on the particles in the suspension.

If the exact particle size or size distribution is unknown, then the measurements must be made at an angle large enough for the diffracted intensity I_0 to be negligible for all particles larger than the smallest size of interest. If this lower size limit is 2 μ for example, and m is still 1.5, then I_0 is less than 10% of I_2 for angles $\theta>45°$, and soon becomes negligible at sizes above the lower limit. Even if the refractive index is unknown within very wide limits, it is possible to choose an angle such that the scattered intensity varies very little with refractive index. At an angle of 40°, for example, I_2 only varies from 0.185 to 0.210 as m varies from 1.4 to 1.8, and I_1 varies from 0.012 to 0.018. If the particles of a suspension are known to have refractive indices in this range and are larger than 2 μ, then their total projected area can be estimated from a light-scattering measurement to within a few percent.

3.2 Extinction Measurements on Transparent Spheres

Suppose extinction measurements with an acceptance angle of $\theta=10°$ are made on the same system of transparent, spherical particles described in Sec. 3.1 above.

The mean value of the diffraction component ΔE_0 of the apparent total reduction in extinction ΔE is found from Fig. 4 in the same way as the scattering due to diffraction was found from Fig. 1; the value is $\Delta E_0=0.827$. The contribution from reflection is $\Delta E_1=0.005$ (Fig. 5) and from transmission $\Delta E_2=0.055$ (Fig. 6). The total observed extinction is therefore $2-\Delta E=2-\Delta E_0-\Delta E_1-\Delta E_2=2-0.827-0.005-0.055=1.11$.

The average screening power of the particles under the condition specified is thus 1.11 times the projected area they offer to the incident beam. For a sparse layer or a dilute suspension of such particles, then, division of the proportion of light lost by the factor 1.11 gives the proportion of the illuminated area covered by the particles. For concentrated suspensions the Lambert–Beer law must be used; $f/f_0=\exp(-Ect)$, where f_0 and f are the light flux per unit cross-sectional area of the beam before and after passing through the suspension of thickness t, and c is the particle projected area per unit volume of suspension.

[10] J. Cartwright and J. W. Skidmore, Ann. Occ. Hyg. 3, 33–57 (1961).

TABLE III. Comparison of intensity coefficients $I_{1,1}(\theta)$ of light scattered by external reflection from transparent and absorbing spheres; direction of polarization in plane containing incident and scattered rays.

Refractive index	Scattering angle 30°	40°	50°	67.4°	80°
1.5	0.016	0.012	0.0091	0.0060	0.0045
$1.5(1-0.5i)$	0.023	0.0194	0.0162	0.0123	0.0102
2.0	0.022	0.018	0.015	0.0113	0.0093
$1.5(1-0.2i)$				0.00712	
1.7				0.0082	
	30°	40°	50°	84.6°	100°
1.1	0.0047	0.0025	0.00146	0.000353	0.000225
$1.1(1-0.5i)$	0.0209	0.0169	0.0136	0.00683	0.00212
1.6	0.0174	0.0136	0.0105	0.0052	0.0039
$1.1(1-0.2i)$				0.00186	
1.3				0.00202	

At 67.4° and 84.6°, $I_{1,2}(\theta)=0$ (direction of polarization normal to plane containing incident and scattered rays) for $m=1.5$ and 1.1, respectively.

In practice the exact size or size distribution of the particles whose extinction is being measured is often unknown. The acceptance angle must then be kept so small that $\Delta E=0$, i.e., $E=2$, for all appropriate particle sizes. For example, if the largest particle diameter of interest is 10 μ and $\lambda=0.5$ μ, then, by limiting θ to 0.3°, we have $\Delta E_0=0.026$. ΔE_1 and ΔE_2 are negligible whatever the refractive index, and so using $E=2$ the total particle surface area may be found fairly accurately.

The use of such small angles and the consequent practical difficulties may be avoided if a greater error is tolerable. When z increases above 3, ΔE_0 changes only slowly from 0.8 to 1.0 (Fig. 4), i.e., if the acceptance angle is made large enough to collect nearly all the light diffracted by all particles larger than the minimum size of interest, then taking $\Delta E_0=1.0$ causes an underestimate of particle surface area never worse than 20%. If $\theta=13.9°$, for example, $\Delta E_0>0.8$ for all particles larger than 2 μ diam. If there is also an upper limit of particle size, say 10 μ, which in this case gives $z=15$, $\Delta E_0=0.95$, then taking $\Delta E_0=0.9$ would cause an error in estimated surface area of only a few percent. At angles as large as this ΔE_1 and ΔE_2 are not negligible but can be estimated well enough from an approximate knowledge of the refractive index. At $\theta=13.9°$, for example, $\Delta E_2<0.1$ for $m>1.6$, and $\Delta E_1<0.01$ for $m<2$.

3.3 Moderately Absorbing (Black) Spheres

The calculations apply to particles which are spherical and transparent. Particles with moderate absorption coefficients, i.e., $k>0.1$, and with diameters larger than four wavelengths of light, absorb most of the light entering them so that the transmitted components $I_2(\theta)$ and $\Delta E_2(\theta)$ may be neglected. [The ratio of trans-

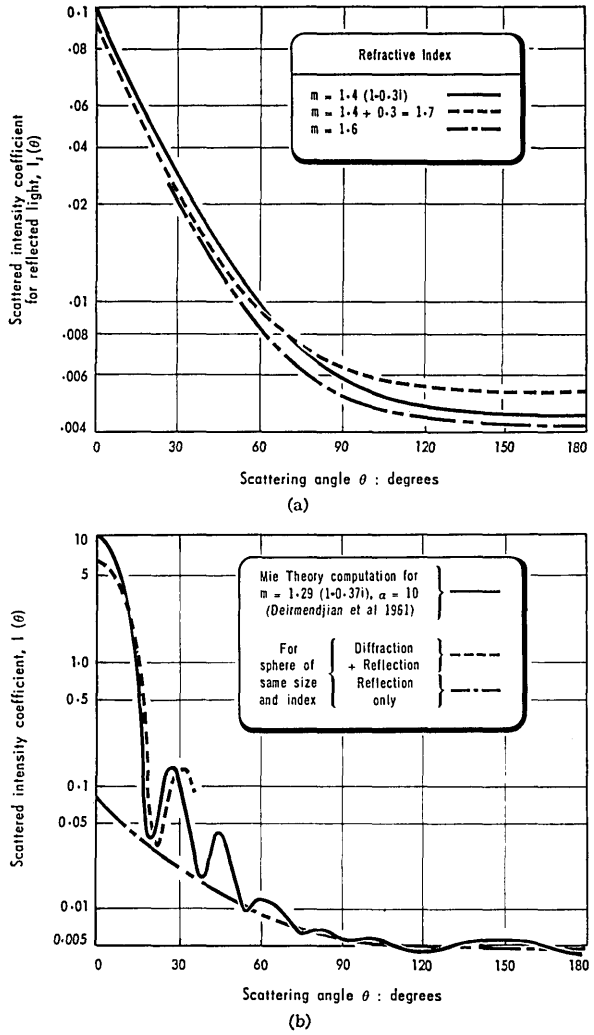

FIG. 7. Computations for moderately absorbing spheres. (a) Approximation of reflection scattering by absorbing spheres of refractive index $m_0(1-ik)$ by calculation for transparent spheres of refractive index (m_0+k). (b) Comparison of scattering by a single moderately absorbing sphere on the Mie theory and the diffraction + reflection approximation.

mitted to normally incident flux with a plane-parallel slab of thickness t and absorption coefficient k is $\exp(-4\pi m_0 kt/\lambda)$.]

The reflected intensities $I_{1,1}(\theta)$ and $I_{1,2}(\theta)$ may be computed from the same exact formulae (2) and (3) as before, using a complex index of refraction $m=m_0(1-ik)$, but the calculation is now much more laborious. It turns out empirically, however, that over a useful range of angles, refractive indices, and absorption coefficients, $I_{1,1}(\theta)$ for $m=m_0(1-ik)$ is roughly the same as for $m=m_0+k$. The larger m and the smaller k, the better the approximation. Some values calculated from the Mie theory are given in Table III. If $m=1.5(1-0.5i)$, for example, the approximation is in error by -5% at 30°; if $m=1.1\ (1-0.5\,i)$ the error is -17% at 30°.

This simple behavior is not followed by $I_{1,2}(\theta)$. An increase in k, i.e., in the imaginary component of the refractive index, still produces an increase in $I_{1,2}(\theta)$ at all angles, whereas an increase in the real component of refractive index only produces a systematic increase in $I_{1,2}(\theta)$ at angles larger than where the zero in $I_{1,2}(\theta)$ occurs with transparent spheres (Sec. 2.3). At smaller angles, however, the rate of variation of $I_2(\theta)$ with refractive index close to the forward direction is small, and $I_2(\theta)\ll I_{1,1}(\theta)$ away from the forwards and backwards directions, so that the approximation is not affected appreciably. In Fig. 7(a) the angular distribution of the reflected light for moderately absorbing spheres of refractive index 1.4 $(1-0.3\,i)$ is seen to be approximated very well, for angles up to 90°, by the distribution for refractive index $1.4+0.3=1.7$, and fairly well for angles up to 180°.

In scattering measurements from moderately absorbing spheres, $I_{1,2}(\theta)$ may if desired be suppressed by a polarizing device arranged so that only light polarized in the plane containing the incident and scattered ray can reach the receiver.

Using then the transparent-particle graphs (Fig. 5) for $\Delta E_1(\theta)$, with m replaced by (m_0+k), to choose an acceptance angle such that $\Delta E_1(\theta)$ is small it should be possible to interpret extinction measurements on moderately absorbing spheres without appreciable error, since at angles up to 50° $I_{1,2}(\theta)$ is always less than $I_{1,1}(\theta)$ and $\Delta E_1(\theta)$ is small compared with the diffraction component $\Delta E_0(\theta,d)$.

3.4 Totally Reflecting Spheres

Particles with a high value of the absorption coefficient k are strongly reflecting. A perfectly specular-reflecting sphere gives a uniform angular distribution of reflected light of intensity $I_1=1/4\pi$, and then $\Delta E_1=(1-\cos\theta)/2$.

4. COMPARISON WITH MIE-THEORY COMPUTATIONS

4.1 Angular Distribution of Scattered Intensity

Only a few computations on the Mie theory of the angular distribution of scattered intensity for particles larger than one or two wavelengths of light have been made and published, because of the large number of terms involved in the series. Moreover, computations covering a range of particle sizes are needed, in order that the rapid fluctuations in scattered intensity with changing particle size may be smoothed by averaging; at a particle-size parameter $\pi d/\lambda=10$ for example, a 10% change in particle diameter can produce a 10-fold fluctuation in scattered intensity at a given angle.

In all the following calculations we have assumed the particle-size distribution to be such that equal increments in diameter contributed equal increments in particle projected area, as in Sec. 3.1.

The results of Mie theory computations are usually given in terms of the scattered intensity parameters

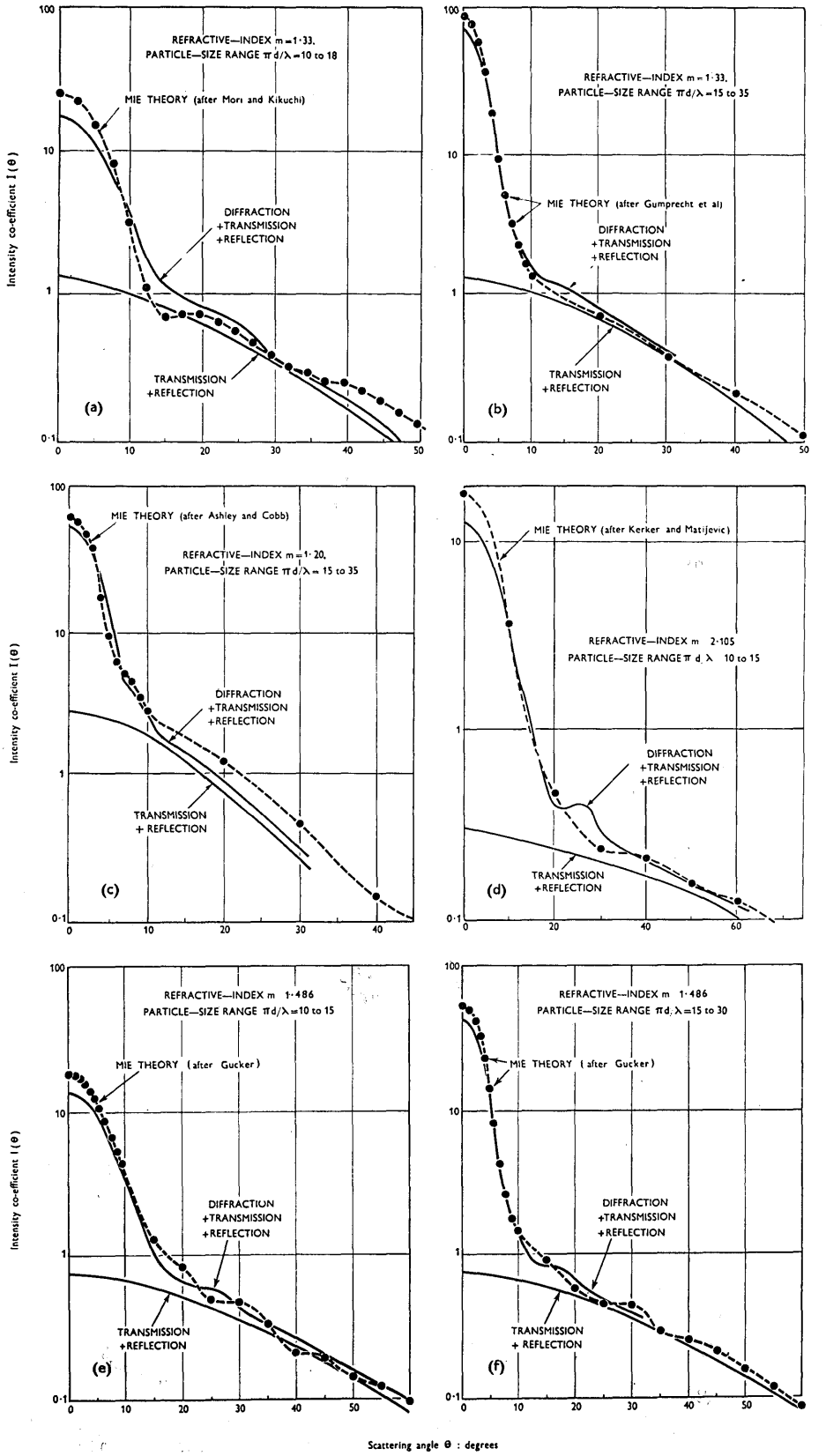

FIG. 8. Comparison of angular distribution of scattered intensity from transparent spheres calculated on Mie theory and on diffraction, transmission, and reflection.

$i_1(\theta,d)$ and $i_2(\theta,d)$, where the particle of diameter d is illuminated by unpolarized light of unit flux per unit beam cross-sectional area. Then $(\lambda^2/8\pi^2)i_1(\theta,d)$ is the component, whose plane of polarization lies in the plane containing the forward beam and the direction of observation, of the flux scattered per unit solid angle at an angle θ to the forward beam. Hence, from our definition of scattered intensity coefficient in Sec. 2.1,

$$I(\theta,d)=\frac{\lambda^2}{8\pi^2}\frac{4}{\pi d^2}[i_1(\theta,d)+i_2(\theta,d)]$$
$$=\frac{1}{2\pi\alpha^2}[i_1(\theta,d)+i_2(\theta,d)],$$

where $\alpha=\pi d/\lambda$.

For transparent spheres of refractive index $m=1.33$, Mori and Kikuchi[11] have computed scattered intensities on the Mie theory for 24 values of the particle-size parameter $\alpha=\pi d/\lambda$ in the range 10 to 18 at angular intervals of $2\frac{1}{2}°$ from $\theta=0°$ to 180°. These intensities have been averaged over this range of particle size and in Fig. 8(a) they are compared with the intensities derived from Figs. 1–3. The Mie intensities lie within $\pm 30\%$ of the approximate ones over the angular range $\theta=5°$ to 45°.

The comparison can be extended to larger particles of refractive index 1.33 by using the Mie theory computations of Gumprecht *et al.*[12] which provide intensities for five values of particle-size parameter α in the range 20 to 40, at angular intervals of 1° from $\theta=0$ to 10° and intervals of 10° from $\theta=20°$ to 180°. Even though the averaged Mie intensities can be based on only five values, in Fig. 8(b) they are seen to agree with the approximate intensities to within $\pm 15\%$ over the angular range $\theta=2°$ to 40°, and to within $\pm 10\%$ over the range $\theta=3°$ to 30°.

Another comparison, for spheres of refractive index 1.20, can be made with the Mie-theory computations of Ashley and Cobb.[13] Their averaged intensities for $\pi d/\lambda=15$, 20, 30, and 35 (they did not compute for 25) are compared with the approximate intensities in Fig. 8(c). The agreement is not so good as in Fig. 8(a) and (b) at larger angles, but is better within the first diffraction maximum. Kerker and Matijevic[14] happened to duplicate a few of Ashley and Cobb's[13] computations, namely $\pi d/\lambda=1$, 2, 3, and 5 at $\theta=90°$. There were large discrepancies for i_2 at $\pi d/\lambda=1$ and for i_1 at $\pi d/\lambda=3$, although there was agreement for the other six values. However, since each point in Fig. 8(c) is the average of eight values and the course of the curve is fairly smooth, Ashley and Cobb's[13] computations seem to be reliable enough for our purpose.

A comparison for spheres of refractive index 2.105, using the Mie-theory computations of Kerker and Matijevic[15] to obtain an average from $\pi d/\lambda=10$ to 15 in increments of 0.2 also shows good agreement with classical optics [Fig. 8(d)]. Another comparison, for spheres of refractive index 1.486, has been made from some of Gucker and Rowell's[16] computations which have been made available to me, for the size ranges $\pi d/\lambda=10$ to 15 and 15 to 30, in both cases with increments of 1 in $\pi d/\lambda$. Again, there is good agreement with the classical optics calculations [Figs. 8(e) and (f)].

More extensive comparisons with the Mie theory will be possible when the completed computations of Penndorf[17] are published, covering refractive indices $m=1.33$, 1.40, 1.44, 1.486, and 1.50 for the particle-size range $\pi d/\lambda=0$ to 30 in intervals of 0.1, and in small angular increments.

To estimate whether the sum of the diffracted and externally reflected intensity was likely to be in agreement with Mie-theory computations of scattering by moderately absorbing (i.e., black) particles, a comparison has been made between the Mie-scattering diagram published by Deirmendjian *et al.*[18] for a single sphere of size $\alpha=10$, refractive index $1.29(1-0.37\,i)$, and the angular scattering distribution calculated from diffraction and reflection [Fig. 7(b)]. Good agreement is observed even though there has been no averaging out of the details of the Mie scattering distribution by the presence of a range of particle size, as was necessary for the transparent spheres. The suppression of the transmitted light eliminates the complex details due to its interference with the diffracted and reflected components. The strong scattering at angles greater than 90°, due to internal reflections, has also been eliminated by absorption, so that the simple approximation is successful up to 180° for moderately absorbing spheres. Similar behavior appears to be shown by the Mie-scattering diagrams published by Giese[19] and Olaf and Robock[20] and envisaged by Haugen[21] and it is intended to make detailed comparisons when tabulated values are available.

4.2 Reduction in Extinction due to Collection of Some Scattered Light

For transparent spheres the total extinction on the Mie theory rises from 0 to about 4 as $\pi d(m-1)/\lambda$ increases from 0 to about 2.1 and then oscillates with

[11] N. Mori and H. Kikuchi, Bull. Electrotech. Lab. (Tokyo) **22**, 209–224 (1957).
[12] R. O. Gumprecht, N. L. Sung, J. H. Chin, and C. M. Sliepcevich, J. Opt. Soc. Am. **42**, 226–231 (1952).
[13] L. E. Ashley and C. M. Cobb, J. Opt. Soc. Am. **48**, 261–268 (1958).
[14] M. Kerker and E. Matijevic, J. Opt. Soc. Am. **50**, 722–729 (1960).
[15] M. Kerker and E. Matijevic, J. Opt. Soc. Am. **51**, 87–92 (1961).
[16] F. T. Gucker and R. L. Rowell, Discussions Faraday Soc. **30**, 185–191 (1960).
[17] R. Penndorf and B. Goldberg, Geophysical Res. paper No. 45 (1956), U. S. Air Force, Cambridge Research Center.
[18] D. Deirmendjian, R. Clasen, and W. Viezee, J. Opt. Soc. Am. **51**, 620–633 (1961).
[19] R. H. Giese, Z. Astrophys. **51**, 119–147 (1961).
[20] J. Olaf and K. Robock, Staub **21**, 495–499 (1961).
[21] D. A. Haugen, "On the scattering of light by spherical absorbers," S. M. thesis (1953), Department of Meteorology, MIT.

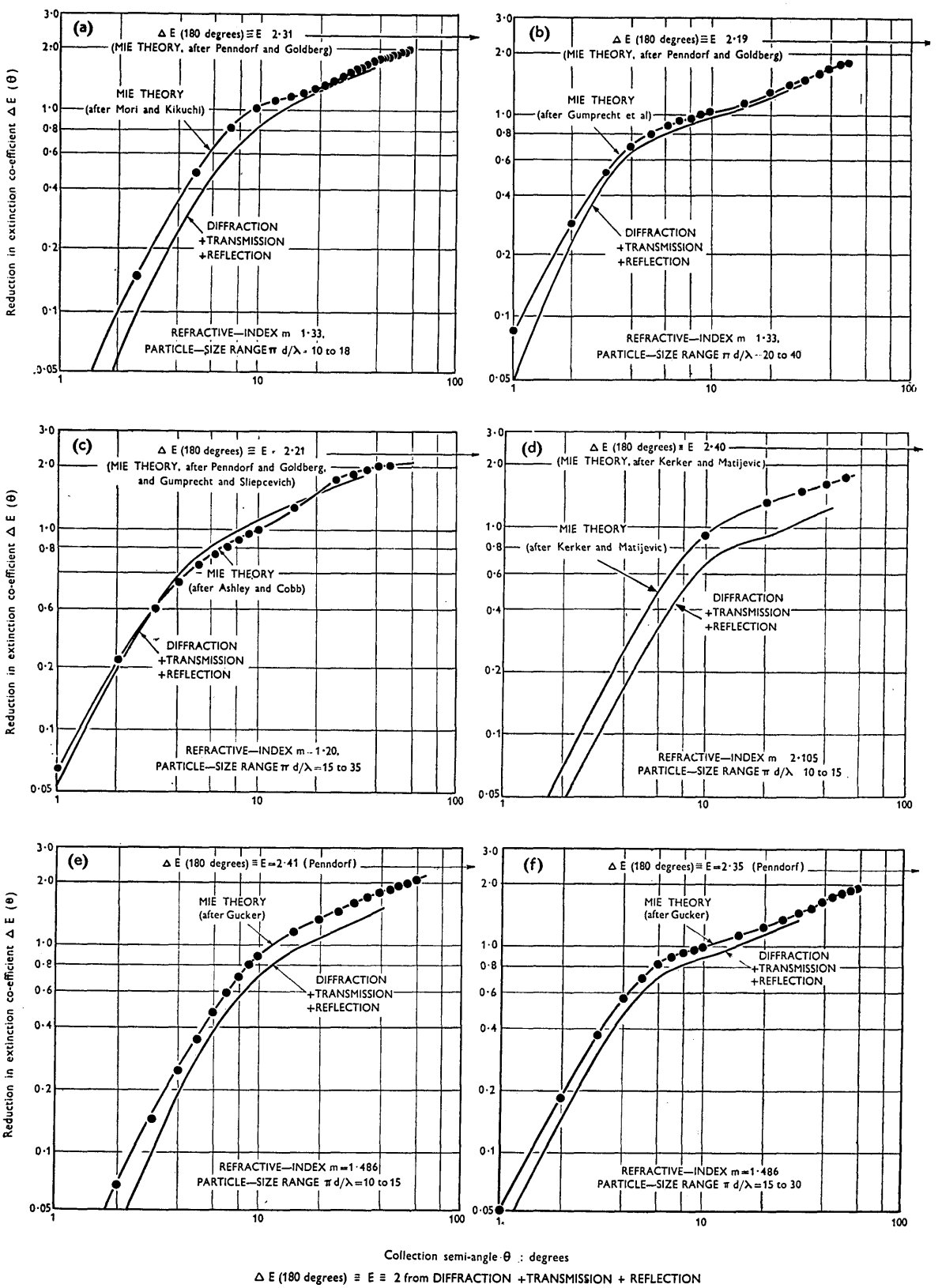

FIG. 9. Comparison of variation in reduction in extinction with collecting angle for transparent spheres calculated on Mie theory, and a diffraction, transmission, and reflection.

diminishing amplitude with further maxima at about $\pi d(m-1)/\lambda = 5.4$, 8.6, 11.7, etc., the minimum values being approximately 2.[6] Since the approximate treatment supposes $\pi d/\lambda > 5$ at least, the particles are usually beyond the first minimum on the extinction curve, and if a particle size range of 2:1 or more is present, the averaged extinction is not much above 2.

The total reduction in extinction $\Delta E(\theta)$ has been derived from each of the Mie-theory intensity-distributions in Fig. 8 by graphical integration. The average intensity in successive small intervals of θ is multiplied by the solid angle contained in each interval to give the total flux (per unit flux geometrically incident on the particle) scattered in that interval; the cumulative total flux then gives the angular variation of $\Delta E(\theta)$ for these particles on the Mie-theory. In Fig. 9 it is seen to agree reasonably well in most cases with the values of $\Delta E(\theta)$ calculated on the basis of diffraction, transmission, and reflection, read from Figs. 4, 5, and 6.

Some calculations showing good agreement between the reduction in extinction calculated on the Mie theory and on the diffraction approximation have been made by Gumprecht and Sliepcevich[22] for transparent spheres of refractive index 1.20, 1.33, and 1.44 of single particle size down to $\pi d/\lambda = 20$ and for small collection angles. For example, when $m = 1.33$, and $\theta = 7°$, the ratio of apparent to total extinction was 0.679 on the Mie theory and 0.631 on the diffraction approximation, even though the absolute values of extinction were 2.14 and 2, respectively. At smaller angles the discrepancy in the ratios was less; and as mentioned above, the total extinctions would come into closer agreement when a range of particle sizes was present.

For absorbing spheres there are instructive Mie-theory computations by Johnson, Eldridge, and Terrell[23] (Figs. 2 and 8) covering spheres of refractive index $1.29(1-ik)$ for a range of absorption coefficients from 0 to ∞, and particle-size parameters up to $\alpha = \pi d/\lambda = 18$ in some cases. By the time k has risen to 0.25 the oscillations in the extinction curve have disappeared; the extinction then rises from 0 to about 2.4 as α increases to 6, and afterward diminishes steadily and asymptotically to 2 as α increases further. Similar behavior is shown in Deirmendjian's computations.[18] Thus calculations of apparent extinction for black spheres on the "diffraction + reflection" approximation should if anything be more successful than those for transparent spheres.

5. CONCLUSIONS

The graphs presented in this paper (Figs. 1 to 6) enable us to make a quick estimation of the scattering and extinction of light by systems of transparent spheres, on the basis of scattering by classical diffraction and by external reflection and transmission of light geometrically incident on the particles. They cover refractive indices from 1.1 to 2.0 and scattering or collection angles up to about 40°. Provided the particles are larger than 3 or 4 wavelengths of light, and a particle size range of about 2:1 is present so that phase effects are averaged out, the scattering and extinction calculated in this way agree well with such direct calculations by the Mie theory as are at present available (Figs. 8 and 9). It is thought that the treatment should also be successful with irregular particles and to some extent with nontransparent particles, such as often occur in airborne dusts in industry.

Inspection of the calculated graphs suggests for example that the proportion of light scattered geometrically through an angle of about 40° by transparent spheres is the same, within $\pm 20\%$, for refractive indices in the range 1.4 to 1.8, which includes many transparent solids; and that the proportion of the light scattered through this angle due to diffraction by particles larger than 2 μ is negligible. Consequently, a measurement of the light scattered through 40° by a polydisperse cloud or suspension of transparent particles larger than 2 μ should give approximately the surface area of particles of all sizes.

An extinction measurement with an acceptance angle less than 1° would give the total surface area of particles within $\pm 10\%$, independent of size, refractive index or degree of transparency, for particle sizes up to 10 μ or more. Extinction measurements are made more easily with wider angles, however; if particles smaller than 2 μ are neglected, a semiangle of about 14° will cause nearly all the diffracted light, but only a small proportion of the geometrically scattered light, to be collected. The latter may be estimated well enough from an approximate knowledge of the particles' refractive index, and hence the projected area of all particles larger than 1 or 2 μ may be derived from the measurement.

ACKNOWLEDGMENTS

This work was carried out at the London School of Hygiene and Tropical Medicine under the direction of Dr. C. N. Davies of the British Medical Research Council. The authors are grateful to Dr. J. McK. Ellison of the Medical Research Council for valuable discussions. The work described forms part of the research undertaken by one of us (J.R.H.) for the degree of Doctor of Philosophy of the University of London[24] and was performed while seconded from the Safety in Mines Research Establishment of the Ministry of Power, Sheffield, England; this was made possible by the cooperation of Mr. H. T. Ramsay, the Director of the Establishment. The illustrations are British Crown copyright.

[22] R. O. Gumprecht and C. M. Sliepcevich, J. Phys. Chem. **57**, 90–95 (1953).

[23] J. C. Johnson, R. G. Eldridge, and J. R. Terrell, Sci. Rept. No. 4 (1954), Dept. of Meteorology, MIT.

[24] J. R. Hodkinson, "Dust measurement by light scattering and absorption," Ph.D. thesis, University of London (1962).